Geography and Sustainability 2 (2021) 281–287

Contents lists available at ScienceDirect

Geography and Sustainability

journal homepage: www.elsevier.com/locate/geosus

Strong direct and indirect influences of climate change on water yield confirmed by the Budyko framework

Hui Yang[1,2], Hao Xu[1], Chris Huntingford[3], Philippe Ciais[1,2], Shilong Piao[1,4,5,*]

[1] Sino-French Institute for Earth System Science, College of Urban and Environmental Sciences, Peking University, Beijing 100871, China
[2] Laboratoire des Sciences du Climat et de l'Environnement, CEA CNRS UVSQ, 91191, France
[3] Centre for Ecology and Hydrology, Wallingford, Oxfordshire, OX10 8BB, UK
[4] Key Laboratory of Alpine Ecology, Institute of Tibetan Plateau Research, Chinese Academy of Sciences, Beijing 100101, China
[5] Center for Excellence in Tibetan Earth Science, Chinese Academy of Sciences, Beijing 100085, China

HIGHLIGHTS

- We attribute recent global changes in runoff and landscape parameter changes.
- Changing climatic characteristics are the primary drivers of global runoff change.
- Indirect effects of climate change on runoff occur through altering plant properties.
- Runoff is sensitive to landscape parameter changes in the transitional region.

GRAPHICAL ABSTRACT

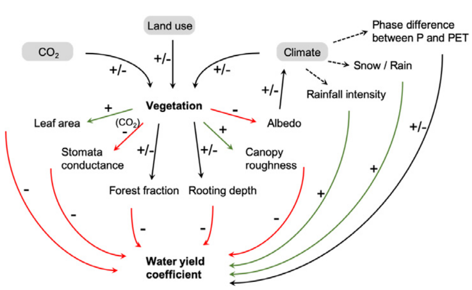

ARTICLE INFO

Article history:
Received 15 July 2021
Received in revised form 19 October 2021
Accepted 3 November 2021
Available online 16 November 2021

Keywords:
Water cycle
Climate change
Atmospheric CO_2
Land cover change
Runoff

ABSTRACT

Research findings concerning the main processes influencing water resources differ substantially, and so the topic remains controversial. Recent studies indicate that the changes in water yield, expressed through the *n*-parameter of Budyko framework, are associated with vegetation coverage changes. Here, we use runoff measurements and outputs from 13 dynamic global vegetation models, to investigate the underlying drivers of the *n*-parameter changes. Unlike previous studies, we instead find that climate change is the primary driver of adjustments on water resources. Changing climatic characteristics, particularly the intensity and seasonality of rainfall, modulates the runoff generation process. Indirect effects of climate change occur through altering vegetation properties, which in turn also impact river flow. We also find that in the arid and sparse vegetation regions, water yield is more sensitive to changes in *n*-parameter. Thus, the Budyko framework provides a reliable parameter-sparse representation of runoff changes, and reveals that terrestrial water cycle is changing substantially under climate change. This climate forcing requires on-going investigation to generate more refined and reliable projections of future water availability.

1. Introduction

Water is an essential resource for maintaining the terrestrial biosphere and many facets of human society. However, modern industry, irrigated agriculture, hydropower, food productivity and economic prosperity are highly vulnerable to the water scarcity (Schewe et al., 2013). The water yield coefficient, referred to as the proportion of gross water resource to precipitation, characterizes the potential of precipitation to transform into water resources. Yet changes in water yield are governed by multiple interactions between the atmosphere and the land surface, and display significant spatial heterogeneity and uncertainties (Milly et al., 2005; Dai et al., 2009). Earth system models (ESMs), which represent the current knowledge of underlying physics and interaction between different climate processes, are widely used to predict historical and projected future changes in water yield (Jiménez Cisneros et al., 2014), but require a vast amount of computing resources. Furthermore, the complexity of ESMs can make it difficult to pick apart the underlying physical processes. For this reason, simpler approaches or models which can capture the salient features of parts of the climate system, such as

* Corresponding author: Shilong Piao
E-mail address: slpiao@pku.edu.cn (S. Piao).

https://doi.org/10.1016/j.geosus.2021.11.001

Budyko framework, are experiencing a revival for both predictive and conceptual analyses.

The Budyko framework is a well-established, empirically verified theory model. It describes the steady-state hydrological partitioning (i.e., Q/P or E/P) as a function of the aridity index, AI, and the curvature parameter n (Choudhury, 1999; Yang et al., 2008). The equation is:

$$\frac{E}{P} = 1 - \frac{Q}{P} = \frac{\mathrm{AI}}{\left[1 + (\mathrm{AI})^n\right]^{1/n}} \tag{1}$$

The aridity index, AI, is the ratio between potential evapotranspiration (PET) and precipitation (P). In Eq. 1, AI characterizes the local hydrothermal conditions and operates as the primary modelled control on the partitioning of precipitation to evapotranspiration (E/P), or water yield coefficient (Q/P). The change in terrestrial water storage over the multi-year timescale can often be negligible ($\Delta S \approx 0$), so we can set the water yield coefficient as one minus E/P, as shown in Eq. 1.

The Budyko framework is widely used to assess or predict the variability of the regional and global water yield coefficient (Q/P) response to changes in aridity index (AI). AI provides the physical limits of atmospheric water supply (i.e., P) and water demand (i.e., PET). Such limits are important as ilustrated, for example, by Berghuijs et al. (2017) through a global sensitivity assessmentwhich showed a high sensitivity of runoff to precipitation over the 83% of the global land cover. However, there is not a single invariant mapping between the driver of aridity index and runoff response, requiring geographically varying additional parameterisation. The Budyko framework places all other processes in a spatially-dependent bulk parameter n, which acts as a second control on the water yield coefficient and is frequently referred to as a proxy of terrestrial water retention. The importance of obtaining the current value of parameter n in the Budyko framework is identified (Donohue et al., 2007), however no conclusive assessment on its magnitude for different locations, and on land surface processes determining its alteration exists.

A vast set of land processes, such as vegetative properties, soil conditions, topographic characteristics, and climatic conditions (e.g., seasonality of P and PET, and rainfall intensity), can affect parameter n, and thus E/P or Q/P. For example, Milly (1994) used a stochastic model and identified the factors influencing parameter n in the Budyko framework, which include the ratio of water-holding capacity to annual mean precipitation amount, the number of precipitation events, and seasonality of precipitation. Furthermore, many of these influences on n can change in time. Recent regression-based studies report changes in parameter n associated with the response of vegetation to elevated CO_2 concentrations, which may change vegetation coverage, leaf area and stomatal conductance as well as triggering changes in rainfall intensity and seasonality (Li et al., 2013; Zhang et al., 2016; Gudmundsson et al. 2017; Yang et al., 2018).

In this study, we collect hydrological measurements from 41 large basins worldwide and analyse the data in parallel with outputs from 13 dynamic global vegetation models run globally. Based on the Budyko framework, we investigate changes in n-parameter and their drivers for the period of 1980-2005. Specifically, we address the following questions:

- How did the parameter n change during the past decades? Were these changes similar or divergent over different river basins and regions?
- What were the major drivers of the parameter n changes? Specifically, how did the environmental factors of elevated CO_2 concentration, climate change and land use change impact parameter n either directly or indirectly through altering vegetation properties?
- How did the parameter n impact water yield, and what is the differential sensitivity of water yield to parameter n between dry and wet regions?

2. Material and methods

2.1. Linking changes in parameter n of the Budyko framework to variations in water yield

In the Budyko framework (Eq. 1), the quantities of P, Q, and PET are available from either observations or models, allowing the derivation of time-evolving parameter n. Here we focus on understanding recent changes in parameter n during the period of 1980-2005 given the substantial availability of data. The changes in n are calculated as the difference between the second and first 13-year period (i.e., $\Delta n = n_{1993-2005} - n_{1980-1992}$).

We use a first-order Taylor expansion of the Budyko equation to quantify the direct contributions of changes in AI versus n-parameter on the water yield coefficients.

$$\Delta\left(\frac{Q}{P}\right) = \frac{\partial\left(\frac{Q}{P}\right)}{\partial \mathrm{AI}}\Delta \mathrm{AI} + \frac{\partial\left(\frac{Q}{P}\right)}{\partial n}\Delta n \tag{2}$$

From Eq. (2), partial derivatives to express the sensitivities of the water yield coefficient are:

$$\frac{\partial\left(\frac{Q}{P}\right)}{\partial \mathrm{AI}} = \frac{1}{(1+\mathrm{AI}^n)^{1/n}}\left[\frac{\mathrm{AI}^n}{n(1+\mathrm{AI}^n)} - 1\right] \tag{3}$$

$$\frac{\partial\left(\frac{Q}{P}\right)}{\partial n} = -\frac{\mathrm{AI}}{n^2}\frac{\ln(1+\mathrm{AI}^n)}{(1+\mathrm{AI}^n)^{1/n}} + \frac{\mathrm{AI}^n}{(1+\mathrm{AI}^n)^{1/n+1}} \tag{4}$$

Based on Eq. 4, changes in water yield coefficients have two components (i.e., equation terms) in the response to parameter n induced changes, and when scaled with Δn:

$$\Delta\left(\frac{Q}{P}\right)_n = \frac{\partial\left(\frac{Q}{P}\right)}{\partial n}\Delta n = \left(-\frac{\mathrm{AI}}{n^2}\frac{\ln(1+\mathrm{AI}^n)}{(1+\mathrm{AI}^n)^{1/n}} + \frac{\mathrm{AI}^n}{(1+\mathrm{AI}^n)^{1/n+1}}\right)\Delta n \tag{5}$$

2.2. River discharge measurement and climate data

River discharge measurements for 41 large basins around the world were collected from the gauging stations close to the mouth of rivers (Supplementary Fig. 1). All the selected rivers have more than 80% data availability for the 1980-2005 study period . The large rivers were selected assuming basin areas above 100,000 km^2. These measurements were obtained from the river discharge archive, collected by Dai et al. (2009) and the China Statistical Yearbook (Bureau, 2000). For the precipitation (P) and potential evaporation (PET) data, we used the observation-based gridded data for period 1980-2005 and from the Climate Research Unit (CRU v3.25; Harris et al., 2014).

2.3. Dynamic Global Vegetation Models (DGVMs) simulations

To investigate the factors driving changes in retention parameter n, we used outputs from simulations by 13 DGVMs held in the TRENDY v6 project ensemble (Sitch et al., 2015; Le Quéré et al., 2018). These DGVMs are CABLE, CLM4.5, DLEM, ISAM, JSBACH, JULES, LPJ-GUESS, LPX, LPX-Bern, ORCHIDEE, ORCHIDEE-MICT, SDGVM and VISIT models. For each DGVM, one control simulation with no change in the drivers and three factorial simulations are available to isolate the individual contributions of elevated CO_2 concentration, climate change and land cover change. Using the TRENDY notation, we used the following simulations: (S0) time-invariant CO_2, climate and land-cover; (S1) time-invariant climate and land-cover, varying CO_2 only; (S2) time-invariant land-cover, varying CO_2 and climate; and (S3) varying CO_2, climate and land cover. The CO_2 concentration forcing data are derived from ice-core measurements merged with NOAA annual CO_2 records. Climate forcing data were derived from the CRU-NCEP v7 dataset, which

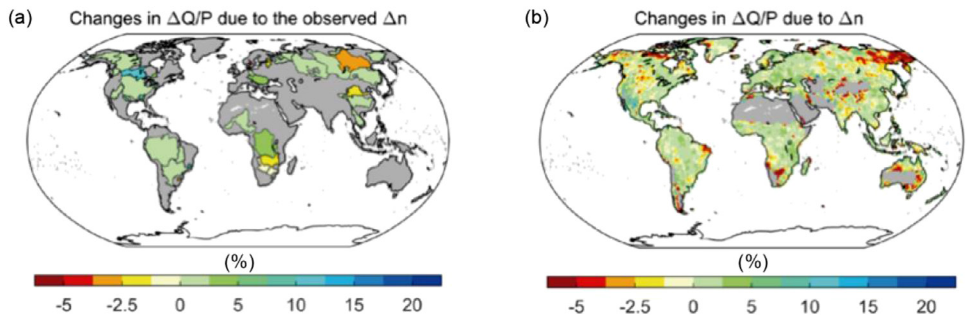

Fig. 1. The effect of *n*-parameter changes on water yield. (a) Spatial patterns of the changes in $\Delta Q/P$ for 41 major river basins, and as caused by the observed changes in the *n*-parameter between the two periods 1993-2005 and 1980-1992. These are retention-based changes alone, i.e., not including any additional changes due to altered AI drivers. (b) Same as (a), but using the multi-model ensemble mean of the TRENDY simulations.

is based on CRU monthly climatology and from the NCEP data to generate the daily and diurnal variability. The forcing data of land-cover change is from the LUH2v2h reconstruction (Hurtt et al., 2011), which provides annual fractional data on primary vegetation, secondary vegetation, and the transitions between land cover states. Typically, models use different rules to translate land cover to different plant functional types (PFTs) (Yang et al., 2020). Using modelled quantities of *P, Q*, and PET, the values of the *n*-parameter are estimated by a non-linear fitting of Eq. (1). This fitting derives the changes in the *n*-parameter due to elevated CO_2 concentration, climate change and land cover change, which are separated by the differences between simulations, i.e., S1−S0, S2−S1, and S3−S2. Note that the effect of climate change represents the direct impact of the observation-based climatic condition changes (e.g., alternation to temperature, precipitation, radiation, humidity and wind speed). Since the climate change signal is predominantly triggered by elevated atmospheric CO_2 concentration, the effect of climate change can be considered as an indirect effect of raised CO_2 concentrations.

3. Results

3.1. *The contributions of* n *to the water yield coefficients*

Eq. (4) allows the calculation of the specific *n*-related impact on the partitioning of precipitation into runoff, expressed by the water yield coefficient. Our calculations are performed for the period of 1980-2005, using both basin-scale measurements and the gridded model outputs, as described in Section 2. Several large catchments, for example, the Congo and Amazon in the wet tropics, Mississippi and Colorado-AR in the United States and the Elbe rivers in Europe, show that recent changes in the *n*- parameter lead to an increase in the water yield coefficients by more than 10% (Fig. 1(a)). In contrast, a few catchments, such as the Zambezi in Africa and the Yellow River in China flowing through arid areas, as well as the Lena in Russia, Gota and Vuoksi in Europe, show changes in parameter *n* which caused a decreased water yield coefficient. We repeat the same analysis, but instead using the inter-DGVM mean gridded river runoff from the TRENDY DGVMs (Fig. 1(b)). Similar to the basin-scale data-based results, the modelled water yield coefficients in wet tropics, most parts of the United States (except northern mountain areas) and Europe, tend to increase caused by changes in the *n* parameter. The opposite is that in dry tropics, northeast China, eastern Siberia, northern Canada and Alaska, the modelled changes in the *n*-parameter lead to a decrease in water yield coefficients. The similarities observed between Fig. 1(a) and Fig. 1(b) provide evidence of good predictive skill by current DGVMs.

3.2. n *changes and contribution from environmental factors*

The importance of changes in *n*-parameter (Δn) in adjusting the water yield is established in Fig. 1. We now identify and explore the individual environmental factors driving these changes in *n*. The observed Δn among the 41 river basins are shown in Fig. 2(a). The magnitude of changes in *n*-parameter range from –0.41 in the Doce River to 0.46 in the Jacui River. Δn are generally larger at the tropical river catchments compared to those at the mid and high-latitudes (ranging from –0.24 in the Moose River to 0.22 in the Yellow River). In the tropics, positive changes of *n*- parameter are more likely to occur in the wet tropical catchments, while negative changes are in dry ones. Over the mid- and high-latitudes, most catchments show positive *n*-parameter changes during the study period. The changes in *n*-parameter of river basins are also estimated using the modelled runoff from DGVMs, forced with the observation-based *P* and PET data. The results show that the magnitude and spatial variability of observed *n*-parameter changes for the 41 large catchments can be well reproduced by the multi-model ensemble mean of DGVMs (MMEM) ($R^2 = 0.84$; RMSE = 0.07) (Fig. 1(b)). This good predictive capability implies that the ensemble mean of TRENDY v6 models is likely appropriate for the analysis of investigating the influence of the individual component drivers of the *n*-parameter changes, also for the period 1980-2005.

Factorial numerical simulations can help separate the individual contributions of elevated CO_2, climate change, and land-use change to Δn (Fig. 2(c)-(d)). Our results show that, at the river basin scale, climate change is the dominant driving factor of the changes in *n*-parameter for 26 out of 41 large catchments during 1980-2005. The effects of climate change are mainly negative (i.e., decrease the *n*-parameter) for most catchments at the mid- and high- latitudes, except, notably, for the Gota and Vuoksi rivers in Russia. Climate change also decreases *n* for the Amazon and Doce rivers in South America. For a few catchments in the dry tropics, such as Jacui, Okavango and Limpopo, the climate change effect is positive, i.e., increases *n*. Elevated CO_2 concentration is the second most important factor, and its impact on *n* is dominant in 13 out of 41 catchments (e.g., a decrease *n* in the Parana and Congo and an increase *n* in the Kelantan and Lena rivers). Land-use change exerts a much smaller influence on changes in *n*-parameter, although their influence is pronounced in a few specific catchments. In particular, land-use change suppresses *n*-parameter in the Jacui, Limpopo and Zambezi catchments, while enhances *n*-parameter in the Colorado-TX, Nelson and Olenek basins.

To further explore the Δn related processes, we use our dynamic global vegetation models to calculate the simulated grid cell-scale contribution of all forcings, and the individual driving factors, to the *n*-parameter changes. Like our catchment-based assessment, climate change is the main driving factor of parameter *n* changes, corresponding to over 60% of the global land area (excluding Antarctica). The effects of climate change are consistent between DGVMs for many regions (small black dots, Fig. 3(b)). Climate change impacts on *n* are positive in the northern high latitudes and dry tropical regions. In contrast, they are negative in most parts of Europe, the wet tropical South America and Africa (Fig. 3(b)). The effect of elevated atmospheric CO_2 concentration dominates changes in *n*-parameter for 29% of global land area (Fig. 3(c)). The elevated CO_2 concentration has both positive and negative effects on the water yield, through altering vegetation properties, as described schematically in Fig. 4. Our factorial simulations show that, in most parts of the northern high latitudes and wet tropics, the elevated CO_2 concentration tends to favour water yield (corresponding to an *n* decrease) because of reduced transpiration caused by CO_2-induced stomatal closure (Supplementary Fig. 2(b)). In contrast, the elevated CO_2

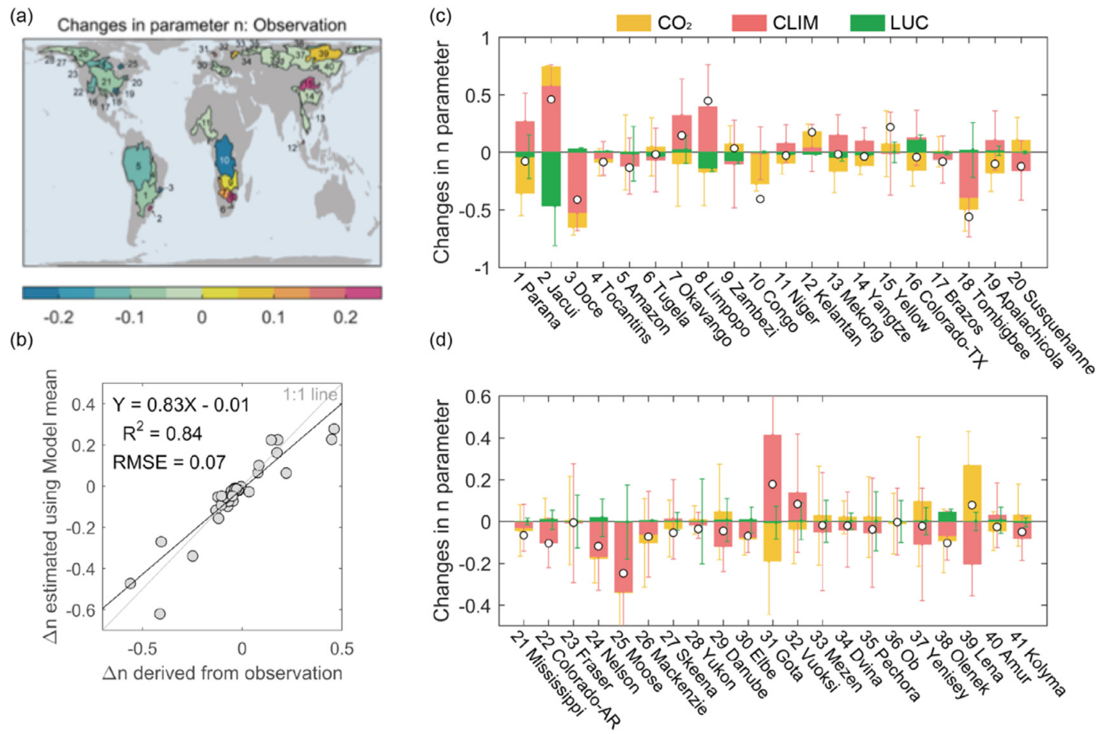

Fig. 2. The attribution of the observed n-parameter changes in large river basins. (a) A map of 41 major river basins (colored) and their parameter n changes (Δn) between two periods: 1993-2005 minus 1980-1992. Parameter n of the Budyko framework is estimated by the measured river runoff and precipitation. (b) Comparison of changes in n-parameter (Δn) fitted using the observation-based Q, P and PET versus Δn fitted using the multi-model ensemble mean. (c)-(d) Different modelled contributions to changes in n-parameter, with Δn derived from simulations (S1-S0), (S2-S1) and (S3-S2). Catchment numbers and names as labelled. (c) For catchments 1-20 and (d) for catchments 21-41, catchment numbers are identical to those marked on map (a). The observation-based Δn are marked as white dots, hence identical values to colors in (a). The error-bars represent the ± standard deviation of Δn from the 13 individual DGVMs.

concentration suppresses water yield (corresponding to an n increase) in southern Europe, western Russia, Mexico, southern South America, and primarily due to increased evaporation (Supplementary Fig. 2(a)). Such evaporation increase is a result of the structural effect of CO_2 fertilization effect overtaking the physiological effect of CO_2 (Piao et al., 2007). The structural effect stimulates photosynthesis and biomass production of C3 plants, leading to their growth and so higher evaporation, while the physiological effect leads to stomatal closure, causing lower leaf-level transpiration. This balance of effects of elevated CO_2 concentration on the n-parameter, unlike for the climate change effect, are much less consistent between models, and may even be opposite in individual model simulations.

Land use change is generally outweighed by climate change and elevated CO_2 concentration impacts in most regions (Fig. 3(d)). However, the influence of land use on the n-parameter is pronounced in parts of the tropical regions where deforestation occurred (Fig. 3(d) and Supplementary Fig. 3). As expected in deforested regions, land use adjusts terrestrial water retention caused by lower forest cover fraction (Fig. 4). The DGVMs show that the losses in tropical forest fraction mainly reduce plant transpiration and canopy interception, increasing the water yield (corresponding to n decrease; Supplementary Fig. 3). Notable, however, is that forest cover fraction in Europe increased during the period 1980-2005, yet such afforestation or reforestation has little effect on the n-parameter and water yield (Supplementary Fig. 3). We suggest this may be due to the young trees being and therefore their limited capability to transpire water due to lower leaf area and root development compared with mature forests (Chiraz, 2013). In a paired catchment study, Brown et al. (2005) found that the response in water yield was slower following afforestation than deforestation because it took longer for trees to reach a new equilibrium of water use.

3.3. *Sensitivity of water yield coefficient* Q/P *to* Δn

After linking recent changes in the n-parameter to three potential drivers (Fig. 3(b)-(d)), we now investigate the sensitivity of the water yield coefficient to the changes in the n-parameter using Eq. 4. With just two drivers and parameters in the Budyko framework (AI and n), this allows for diagrammatic illustration of the full range of the responses of the model (Fig. 5). This presentation of the responses of Eq. (1) shows how the change in water yield coefficients, for a given change in parameter n, depends nonlinearly on the level of aridity index (AI) and the initial value of n-parameter. For instance, given an initial value of parameter n of $n_0 = 2$, then a decrease in n of –0.8 in a wet region with AI = 0.5 causes an increase in Q/P of +0.08 (Fig. 5(a)). However, the same decrease in n of –0.8 in a dry region with AI = 1 leads to a more substantial increase in Q/P of +0.15 (Fig. 5(c)). This finding is generalized in the contour diagram of Fig. 5(b), presenting $\Delta(Q/P) = f(\mathrm{AI}, \Delta n)$ for n_0=2.0. Fig. 5(c) shows that with an increase of aridity index (i.e., AI = PET/P), the sensitivity of Q/P to n-parameter increases rapidly for range 0 < AI < 1.5. However, the sensitivity then switches to decreasing slowly when AI > 1.5. That is, transitional regions, often defined for AI near to 1.5, are very sensitive to n-parameter changes. A second representation is that for a fixed aridity index of AI = 1. For this AI value, a decrease in n of –0.8 and for a low initial value of n_0 = 2 results in an increase in Q/P of +0.15 (Fig. 5(c)). However, the same decrease of –0.8 of parameter n in a region with a high initial value of n_0=3.8 (again AI = 1) leads to a smaller increase in Q/P of +0.04. We expand this representation of response, expressed as $\Delta(Q/P) = g(n_0, \Delta n)$ for AI=2.0 (Fig. 5(d)). Now changes in Q/P in the regions with low n_0 are more sensitive to n parameter changes than that with higher n_0 values. Earlier research implies that the regions with low background retention, n_0, are placed where the majority of precipitation reaches the oceans

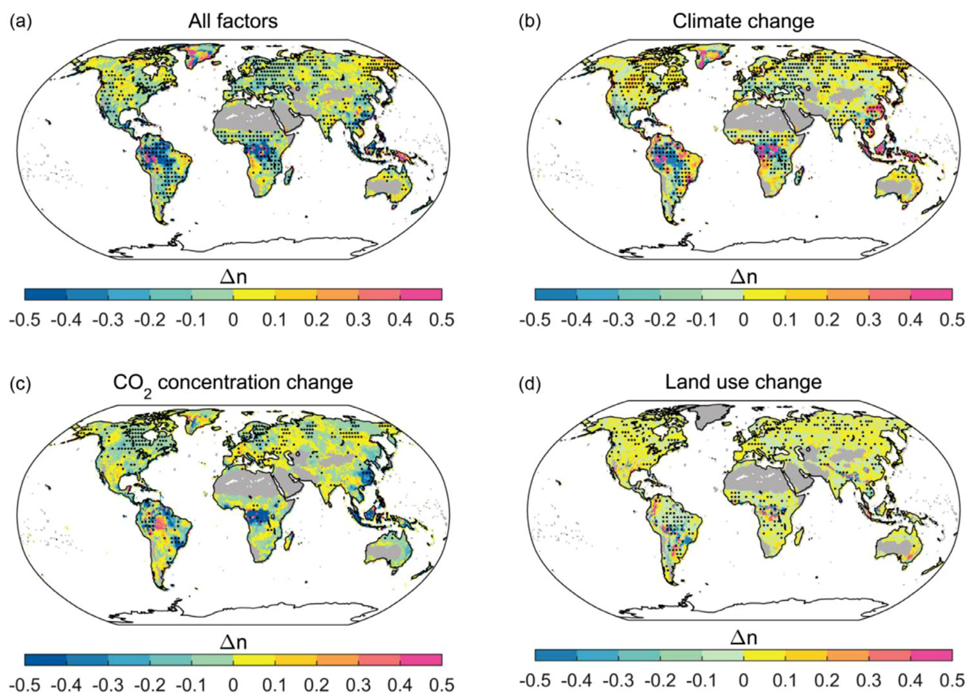

Fig. 3. Global patterns of contributions of individual factors to modeled *n*-parameter changes. (a) The modeled changes in *n*- parameter within the Budyko framework, caused by the combined effects of climate, atmospheric CO_2 and land use(Simulation S3). (b)-(d) Same as (a), but contributions of individual factors to modeled changes in *n*-parameter. Shown are (b) climate change (Simulation S2 – S1), (c) elevated atmospheric CO_2 concentration (Simulation S1 – S0) and (d) land use change (Simulation S3 – S2). All changes are calculated as the difference between two periods of values for 1993-2005 minus 1980-1992, using the DGVM multi-model ensemble mean. Small black dots indicate where more than 80% of individual models show agreement on the direction of changes in *n*-parameter. The grey areas have insufficient data.

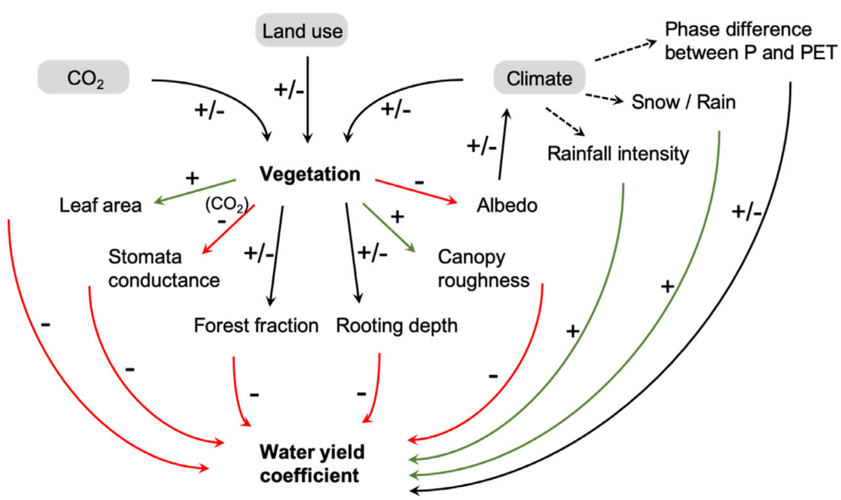

Fig. 4. Conceptual diagram of the possible processes other than the aridity index (AI) influencing water yield coefficient. Positive responses and negative responses arising from vegetation properties and water yield are green and red arrows, respectively. And the processes with both positive and negative responses are colored in black.

via river runoff, and are likely to have low vegetation coverage, low soil infiltration capacity and steep topography (Milly, 1994). The common feature in both contour plots shown in Fig. 5(b) and 5(d) is that changes in Q/P is more sensitive to the decrease of n parameter rather than the increase of n-parameter.

4. Discussion

*4.1. The influence of climate change on parameter-*n *and runoff changes*

Our overall finding is that for recent decades, the most substantial influence on changes in water availability (expressed via water yield coefficient, Q/P) are due to direct climate change. The next most important driver is CO_2 increase, followed by land use impacts. Given the importance of climate change, we discuss the possible climate-related processes listed in conceptual Fig. 4 and impacting water yield, as diagnosed by altering the n-parameter within the Budyko framework. First, key climatic characteristics such as changes to the intensity of rainfall events, the fraction of precipitation falling as snow and seasonal phase difference between P and PET, can all adjust water yield by altering the runoff generation process (Shao et al., 2012; Berghuijs et al., 2017; Padrón et al., 2017). As shown in Supplementary Fig. 1, in wet tropical South America and Africa, the increased intensity and frequency of rainfall, and difference in phase of P and PET tend to increase water yields (corresponding to a decrease in the value of the n parameter). This rise in runoff is produced by soil saturation or insufficient infiltration capacity, lowering soil water retention during days with high precipitation (Padrón et al., 2017). For regions experiencing substantial snow cover, global warming will decrease the fraction of precipitation falling as snow (Supplementary Fig. 1(e)). This change to more rainfall could decrease the water yield (corresponding to n increase). Second, the indirect effects of climatic change will alter vegetation properties, also changing water yield. Adjustment to vegetation is mainly through changing LAI (Zhu et al., 2016). Our factorial simulations show positive and direct effects of climate on LAI in dry tropics and almost all northern high latitudes. For such locations, there is an enhancement of transpiration and evaporation due to extra leaf cover offsetting any CO_2-induced stomata closure, leading to lower water yields (corresponding to an n increase). In contrast, climate-induced LAI decreases in the wet tropics, most parts of Europe and eastern USA (Supplementary Fig. 1) cause a decrease in ET and increase in water yield under climate change (n decrease).

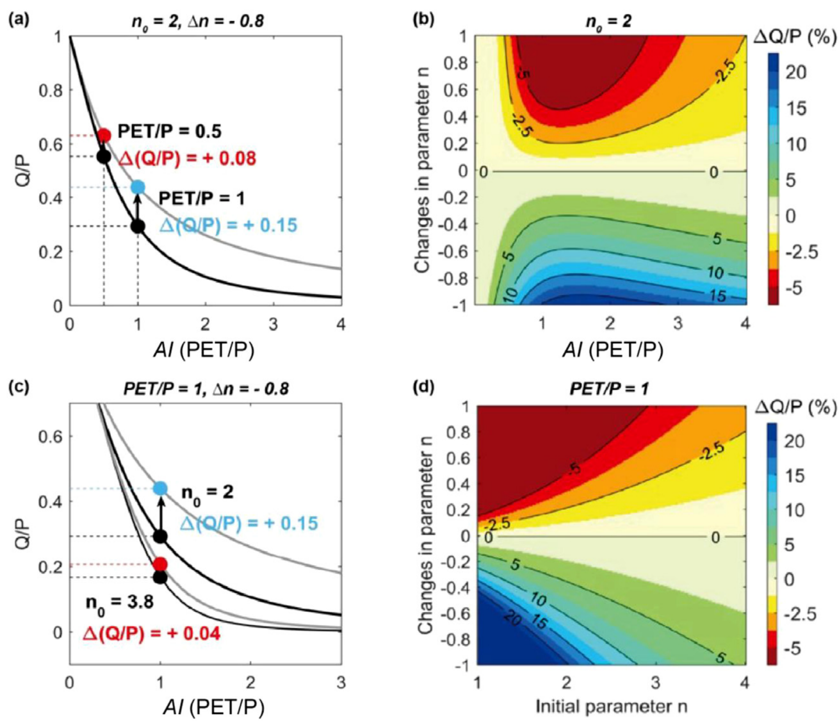

Fig. 5. The variations in the sensitivity of water yield coefficient to n-parameter changes. (a)(b) For a given initial parameter n (e.g. n_0 = 2) and under different levels of aridity index (AI), curves and contour diagrams show the effects of changes in parameter n on water yield coefficient [$\Delta(Q/P)$] (as %). (c)(d) Same as (a)(b), but for a given aridity condition (e.g. AI = 1) and under different levels of initial n-parameter (n_0).

4.2. *Regional hotspots affected by the* n*-parameter changes*

The theoretical vulnerability of water yield coefficients to changes in surface conditions, expressed via altered values of parameter n changes, are illustrated in Fig. 5. The hotspot regions are placed where the water yield coefficients are very sensitive to parameter n changes, which is in general for water-limited and sparse vegetation regions (with 1 < AI < 2 and/or low n_0 value). This sensitivity finding implies that any changes to the aridity index in such locations may not be the only factor determining changes in water yields. Instead, for these places, alterations to land surface properties including vegetative dynamics, soil conditions, topographic characteristics, may adjust retention and thereby the n-parameter. In these circumstances, the Budyko framework predicts large runoff changes that are not caused by AI alone. This analytical result is similar to the findings of the recently published dryland expansion studies, e.g., Lian et al. (2021) and Berg and McColl (2021). Those researchers suggested that the increased atmospheric aridity would not exacerbate soil moisture and runoff deficits when additionally considering the role of structural and physiological responses of vegetation under elevated CO_2 and climate change. Understanding the responses of global water yields to environmental condition changes are fundamental to sustainable development under climate change. Our results highlight that linking the climatic and land surface characteristics is essential to understanding and projecting water yield changes, and notably these processes may be more important than direct land-use change.

5. Conclusions

This study analyses in detail the changing response of land water yields, defined as the ratio of runoff to rainfall. Using the parameter-sparse Budyko framework, in parallel with state-of-the-art dynamic global vegetation models for which there are factorial simulations, it is found that climate change is the primary driver of changes to the n-parameter . The n-parameter characterises the additional features that affect water yield, beyond simply changes in aridity index (expressed via the AI parameter). The analysis shows that changing climatic characteristics over the last decades, such as rainfall intensity, directly altered the runoff generation process via retention changes, as represented through n. Additional indirect changes are also occurring by altering vegetation properties. The same magnitude of changes of Δn can result in different impacts on water yield coefficients, dependent on the level of aridity index (AI) and the initial value of n-parameter (n_0). In the transitional regions (where 1 < AI < 2), or the locations with low n_0, for example where there is low vegetation coverage, low soil infiltration capacity or steep topography, water yield coefficients are more vulnerable to small changes in n. The results presented highlight the usefulness of a traceable but parameter-sparse model in explaining how changing environmental drivers are adjusting water resources. In particular, features of climate change are altering soil water retention properties, which may impact river runoff by adding to the direct effects of adjusted levels of aridity.

Author contributions

S.P. designed the research. H.Y. performed analysis and created all the figures. H.Y. and S.P. wrote the first draft of manuscript. All authors contributed to interpretation of the results and to the text.

Declaration of interests

The authors declare that they have no known competing financial interests or personal relationships that could have appeared to influence the work reported in this paper.

Acknowledgments

This study was supported by the National Natural Science Foundation of China (Grant No. 41988101). We acknowledge the TRENDY Modeling Group for producing and making available their model output.

Supplementary materials

Supplementary material associated with this article can be found, in the online version, at doi:10.1016/j.geosus.2021.11.001.

References

Berg, A., McColl, K.A., 2021. No projected global drylands expansion under greenhouse warming. Nat. Clim. Change 11 (4), 331–337.

Berghuijs, W.R., Larsen, J.R., van Emmerik, T.H.M., Woods, R.A., 2017. A global assessment of runoff sensitivity to changes in precipitation, potential evaporation, and other factors. Water Resour. Res. 53 (10), 8475–8486.

Brown, A.E., Zhang, L., McMahon, T.A., Western, A.W., Vertessy, R.A., 2005. A review of paired catchment studies for determining changes in water yield resulting from alterations in vegetation. J. Hydrol. 310 (1–4), 28–61.

Bureau, C.S., 2000. China Statistical Yearbook. China Statistical Bureau, Beijing, pp. 10.

Chiraz, M.C., 2013. Growth of young olive trees: Water requirements in relation to canopy and root development. Am. J. Plant Sci. 4, 1316–1344.

Choudhury, B.J., 1999. Evaluation of an empirical equation for annual evaporation using field observations and results from a biophysical model. J. Hydrol. 216 (1–2), 99–110.

Dai, A., Qian, T., Trenberth, K.E., Milliman, J.D., 2009. Changes in continental freshwater discharge from 1948 to 2004. J. Clim. 22 (10), 2773–2792.

Donohue, R.J., Roderick, M.L., McVicar, T.R., 2007. On the importance of including vegetation dynamics in Budyko's hydrological model. Hydrol. Earth Syst. Sci. 11 (2), 983–995.

Gudmundsson, L., Greve, P., Seneviratne, S.I., 2017. Correspondence: Flawed assumptions compromise water yield assessment. Nat. Commun. 8, 1–3.

Harris, I., Jones, P.D., Osborn, T.J., Lister, D.H., 2014. Updated high-resolution grids of monthly climatic observations-the CRU TS3.10 Dataset. Int. J. Climatol. 34 (3), 623–642.

Hurtt, G.C., Chini, L.P., Frolking, S., Betts, R.A., Feddema, J., Fischer, G., Wang, Y.P., 2011. Harmonization of land-use scenarios for the period 1500–2100: 600 years of global gridded annual land-use transitions, wood harvest, and resulting secondary lands. Clim. Change 109 (1), 117–161.

Jiménez Cisneros, B.E., Oki, T., Arnell, N.W., Benito, G., Cogley, J.G., Döll, P., Nishijima, A., 2014. Freshwater resources. In: In: Feild, C.B., Barros, V.R., Dokken, D.J., Mach, K.J., Mastrandrea, M.D. Bilir, T.E., Chatterjee, M., Ebi, K.L., Estrada, Y.O., Genova, R.C., Girma, B., Kissel, E.S., Levy, A.N., MacCracken, S., Mastrandrea, P.R., White, L.L.(Eds.), Climate Change 2014: Impacts, Adaptation and Vulnerability. Part A: Global and Sectoral Aspects. Cambridge University Press, Cambridge, pp. 229–270.

Le Quéré, C., Andrew, R.M., Friedlingstein, P., Sitch, S., Hauck, J., Pongratz, J., Zheng, B., 2018. Global Carbon Budget 2018. Earth Syst. Sci. Data 10 (4), 2141–2194.

Li, D., Pan, M., Cong, Z., Zhang, L., Wood, E., 2013. Vegetation control on water and energy balance within the Budyko framework. Water Resour. Res. 49, 969–976.

Lian, X., Piao, S., Chen, A., Huntingford, C., Fu, B., Li, L.Z., Roderick, M.L., 2021. Multifaceted characteristics of dryland aridity changes in a warming world. Nat. Rev. Earth Environ. 2 (4), 232–250.

Milly, P.C.D., 1994. Climate, soil water storage, and the average annual water balance. Water Resour. Res 30 (7), 2143–2156.

Milly, P.C.D., Dunne, K.A., Vecchia, V., 2005. Global pattern of trends in streamflow and water availability in a changing climate. Nature 438 (7066), 347–350.

Padrón, R.S., Gudmundsson, L., Greve, P., Seneviratne, S.I., 2017. Large-scale controls of the surface water balance over land: Insights from a systematic review and meta-analysis. Water Resour. Res. 53 (11), 9659–9678.

Piao, S., Friedlingstein, P., Ciais, P., de Noblet-Ducoudré, N., Labat, D., Zaehle, S., 2007. Changes in climate and land use have a larger direct impact than rising CO_2 on global river runoff trends. Proc. Natl Acad. Sci. U.S.A. 104 (39), 15242–15247.

Schewe, J., Heinke, J., Gerten, D., Haddeland, I., Arnell, N.W.N.W., Clark, D.B.D.B., Kabat, P., 2013. Multimodel assessment of water scarcity under climate change. Proc. Natl. Acad. Sci. U.S.A. 111 (9), 3245–3250.

Shao, Q., Traylen, A., Zhang, L., 2012. Nonparametric method for estimating the effects of climatic and catchment characteristics on mean annual evapotranspiration. Water Resour. Res. 48 (3), 1–13.

Sitch, S., Friedlingstein, P., Gruber, N., Jones, S.D., Murray-Tortarolo, G., Ahlström, A., Myneni, R., 2015. Recent trends and drivers of regional sources and sinks of carbon dioxide. Biogeosciences 12 (3), 653–679.

Yang, H., Yang, D., Lei, Z., Sun, F., 2008. New analytical derivation of the mean annual water-energy balance equation. Water Resour. Res. 44 (3), 1–9.

Yang, H., Piao, S., Huntingford, C., Ciais, P., Li, Y., Wang, T., Chang, J., 2018. Changing the retention properties of catchments and their influence on runoff under climate change. Environ. Res. Lett. 13 (9), 094019.

Yang, H., Ciais, P., Santoro, M., Huang, Y., Li, W., Wang, Y., Zhu, D., 2020. Comparison of forest above-ground biomass from dynamic global vegetation models with spatially explicit remotely sensed observation-based estimates. Glob. Change Biol. 26 (7), 3997–4012.

Zhang, S., Yang, H., Yang, D., Jayawardena, A.W., 2016. Quantifying the effect of vegetation change on the regional water balance within the Budyko framework. Geophys. Res. Lett. 43, 1140–1148.

Zhu, Z., Piao, S., Myneni, R.B., Huang, M., Canadell, J.G., Ciais, P., Koven, C., 2016. Greening of the Earth and its drivers. Nat. Clim. Change 6 (8), 791–795.